Part C

Inorganic-organic hybrid materials based on mono-copper substituted Phosphotungstate

Organic ligands used:

i. Imidazole

ii. (*S*)-1-Phenyl ethylamine

Chapter 4A

Imidazole functionalized mono-copper substituted phosphotungstate

Synthesis, Characterization, Catalytic Evaluation and Kinetics

Catalysis Letters
https://doi.org/10.1007/s10562-019-02979-1

Hybrid Catalyst Based on Cu Substituted Phosphotungstate and Imidazole: Synthesis, Spectroscopic Characterization, Solvent Free Oxidation of Styrene with TBHP and Kinetics

Anjali Patel[1] · Rajesh Sadasivan[1]

Received: 25 May 2019 / Accepted: 20 September 2019

Abstract
The present work describes the synthesis of a hybrid material based on copper substituted phosphotungstate and imidazole by ligand substitution method along with its characterization by various physicochemical techniques. A physical mixture of the same was also synthesized and characterized to confirm the formation of N→Cu dative bond. The synthesized material was used as a heterogeneous catalyst for the solvent-free oxidation of styrene at an ambient temperature of 60 °C using TBHP as oxidant. The catalyst gives high selectivity towards epoxide with a turn over number of 2185. The synthesized catalyst was recycled and reused for multiple times with negligible loss of catalytic activity. A detailed kinetic study was carried out to understand the role of each component in the reaction and it was found that the reaction followed first order kinetics with respect to individual reactants and an overall second order kinetics.

As mentioned in the introduction, many organic ligands have been used to functionalize POMs, ranging from small alkoxy and aryloxy groups to large amino-acids and polypeptides. Amongst, one of the common organic ligand used are imidazole and its derivatives. Imidazole is a pentacyclic aromatic compound, with two N coordination centres to extend structure. Also, it is a stronger ligand which may offer the possibility to replace the aqua ligand [1]. Many reports are available where POMs are functionalized using imidazole and its derivatives, and due to the vastness of the literature, we will focus on Keggin POMs only.

J-C Tabet et al were the first to synthesize an oxoimido derivative of Keggin type POMs in 2004 [2]. They synthesized Rhenium Phenylimido Tungstophosphate from monolacunary phosphotungstate and $[Re(NPh)Cl_3(PPh_3)_2]$, in acetonitrile and in the presence of NEt_3. Four years later, in 2008, Jun Peng et al have used imidazole as an antenna ligand to functionalize transition metal substituted silicotungstates (where M = Ni, Mn, Co), and thoroughly characterized them [3]. In 2009, a Cu-imidazole complex was used by Zhang and his group to functionalize phosphotungstates by hydrothermal technique [4]. Wang et al, in 2010, synthesized and characterized a hybrid compound based on benzimidazole functionalized silicotungstate [5]. Later, in 2012, Mirkhani et al synthesized hybrid catalysts based on transition metal substituted phosphotungstates (where M = V, Cr, Mn, Fe, Co, Ni, Cu and Zn) and functionalized using 1-*n*-butyl-3-methylimidazolium [6]. They also evaluated the catalytic activity of the compound for oxidation of aromatic alcohols using H_2O_2. In 2014, Xie et al synthesized organic heteropoly acidic salts by partially replacing the protons with sulfonated imidazole derivatives and used for benzylation of anisole with benzyl alcohol [7]. In the following year, Qi et al reported an organic-inorganic hybrid compound based on Co-substituted silicotungstate and imidazole [8]. In 2016, Patel et al have successfully synthesized, characterized an imidazole functionalized Ni-substituted phosphotungstate and evaluated its catalytic activity for the oxidation of styrene

[9]. The above reported hybrid materials have been synthesized either by exchanging available protons of POMs or by co-ordination competition approach. Only one group, Mirkhani et al, has reported functionalization of $PW_{11}Cu$, that too using 1-*n*-butyl-3-methyl derivative of imidazole.

Thus, a literature survey shows that (i) ligand substitution method has not been used for the synthesis and (ii) catalytic applications of the reported is scanty. No reports on oxidation of alkenes using copper substituted POMs functionalized with imidazole. This encouraged us to conduct the study on hybrid material comprising of mono-copper substituted phosphotungstate and imidazole via ligand substitution method, and characterized in detail. The catalytic activity of the synthesized material was evaluated for the oxidation of alkenes using tert-butyl hydroperoxide (TBHP) as the oxidant. Subsequently, tests for leaching and heterogeneity, recycle studies and detailed kinetics of the reactions were also carried out.

EXPERIMENTAL

Materials.

All chemicals used were of A.R. grade. Phosphotungstic acid, Copper chloride dihydrate, Cesium chloride, Imidazole, Sodium hydroxide, Styrene, 70% TBHP and Dichloromethane were obtained from Merck. Cis-cyclooctene was obtained from Spectrochem India Pvt. Ltd., while $NaHCO_3$ was obtained from SRL, Mumbai. All chemicals were used as received.

Synthesis of hybrid material was carried out in two steps.

I. Synthesis of mono-copper substituted phosphotungstate ($PW_{11}Cu$)

$PW_{11}Cu$ was synthesized by the one-pot method mentioned in chapter 1.

II. Functionalization of $PW_{11}Cu$ ($PW_{11}Cu$-Im).

0.35g (0.1 mmol) of $PW_{11}Cu$ was dissolved in 10 mL water by heating. 10 mg (0.1 mmol) of Imidazole was dissolved 10 mL methanol. The methanolic solution of imidazole was added drop-wise to the hot solution of $PW_{11}Cu$ while stirring. The pH was adjusted to 6.4 using NaOH. The resultant mixture was refluxed for 10 h at 90 ^{0}C, cooled, filtered and dried at 100 ^{0}C. The obtained violet coloured powder was designated as $PW_{11}Cu$-Im (Scheme 1).

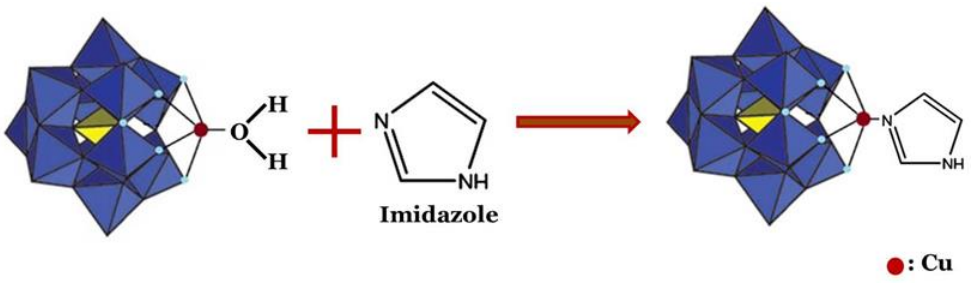

Scheme 1. Functionalization of $PW_{11}Cu$ with Imidazole (Physical texture of synthesized material).

Synthesis of physical mixture ($PW_{11}Cu$+Im).

Physical mixture was synthesized by taking 0.35 g $PW_{11}Cu$ and 10 mg of Imidazole in a mortar followed by grinding them thoroughly with a pestle till fine light violet coloured powder was obtained. This material was designated $PW_{11}Cu$ + Im.

Catalytic reaction

Oxidation of the alkenes was carried out using $PW_{11}Cu$-Im as catalyst, following the method described in chapter 1.

RESULTS AND DISCUSSION

Catalyst Characterization

Gravimetric analysis shows 56.75 wt% of W while volumetric analysis shows 1.82 wt% of Cu, which are in good agreement with the calculated values (W, 56.91 and Cu, 1.90). The synthesized material was also analysed by EDX and the values obtained agree well with the calculated ones. Found: P, 0.96; N, 1.07; W, 56.6; Cu, 1.97; Cs, 18.97. Anal Calc: P, 0.91; N, 0.8; W, 56.91; Cu, 1.90; Cs, 18.64.

The TGA of pure Imidazole shows around 99.7% weight loss at about 100–200 °C indicating degradation of the molecule. $PW_{11}Cu$ (Figure 1a) shows a weight loss of 2.1% between 100 and 150 ^{0}C corresponding to loss of adsorbed water. The TGA curve of $PW_{11}Cu$−Im (Figure 1c) shows an initial weight loss of 1.5% up to 150 ^{0}C due to adsorbed water molecules. This is followed by a weight loss of 3.2% between 250 and 300 ^{0}C which may be attributed to degradation of imidazole. The total number of water molecules was calculated and found to be 7. From the elemental analysis and the TGA, the chemical formula of the isolated complex is $Cs_5[PW_{11}O_{39}Cu(C_3H_4N_2)].7H_2O$.

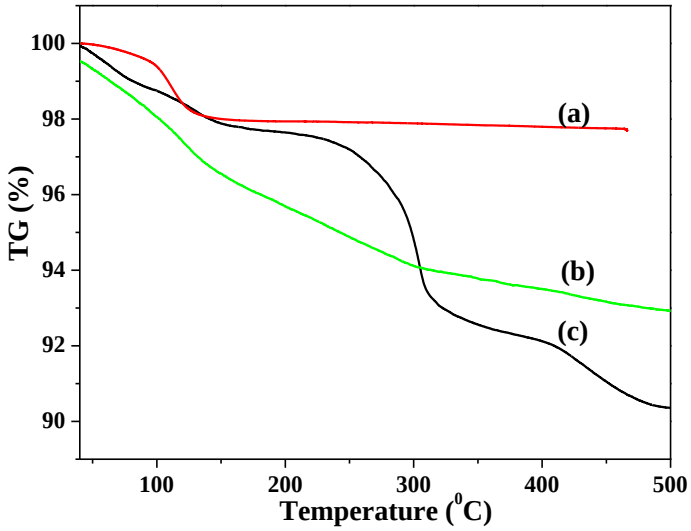

Figure 1. TGA of (a) $PW_{11}Cu$, (b) $PW_{11}Cu$+Im and (c) $PW_{11}Cu$-Im

The TGA of $PW_{11}Cu$+Im (Figure 1b) shows a continuous weight loss of 5.3% up to 250 ^{0}C indicating the loss of adsorbed water molecules as well as the degeneration of Imidazole. Thus the TGA studies indicate the presence of strong interactions between $PW_{11}Cu$ and Imidazole in case of $PW_{11}Cu$-Im, which was further supported by FT-IR studies.

The FT-IR frequencies of $PW_{11}Cu$, Imidazole, $PW_{11}Cu$+Im and $PW_{11}Cu$-Im are shown in table 1. $PW_{11}Cu$ shows characteristic bands at 1103 and 1068; 964; 887 and 821 cm^{-1} and 488 cm^{-1} corresponding to P-O, W=O, W-O-W and Cu-O bonds respectively as described in chapter 1. FT-IR spectra of pure imidazole show band at 3376 cm^{-1} that corresponds to N–H stretching vibration. Along with this, bands at 1486, 1440, 1367, 1325 cm^{-1} correspond to C–N stretching vibrations and bands at 3126, 3040, 2922 cm^{-1} correspond to C–H stretching vibration [10].

Table 1. FT-IR bands

Catalyst	FT-IR Frequencies (cm^{-1})								
	P-O	W=O	W-O-W	Cu-O	Cu-N	C-H	C-C	N-H	C-N
$PW_{11}Cu$	1103 1068	964	887 821	488	-	-	-	-	-
Imidazole	-	-	-	-	-	3126 3040 2922	1593	3376	1486 1440 1367 1325
$PW_{11}Cu$-Im	1101 1068	962	883 810	-	435	3142 2900	1606	-	1490 1400 1310
$PW_{11}Cu$ + Im	1103 1064	964	887 810	-	-	3090 2924 2854	1604	3425	1427 1381 1327 1257

FT-IR of the functionalized $PW_{11}Cu$-Im and physical mixture $PW_{11}Cu$+Im, show the characteristic bands of both $PW_{11}Cu$ as well as imidazole. However, in case of $PW_{11}Cu$-Im, the Cu-O and N-H bands disappear and a new band is observed at 435 cm^{-1}, which is attributed to the Cu-N stretching vibrations [11]. On the other hand, it is interesting to note that N–H band does not disappear, while Cu–N band is not observed in case of the physical mixture. This confirms that there is no formation of chemical bond between $PW_{11}Cu$ and Imidazole. The slight shift in FT-IR bands of $PW_{11}Cu$-Im also validates the successful functionalization of $PW_{11}Cu$ with Imidazole.

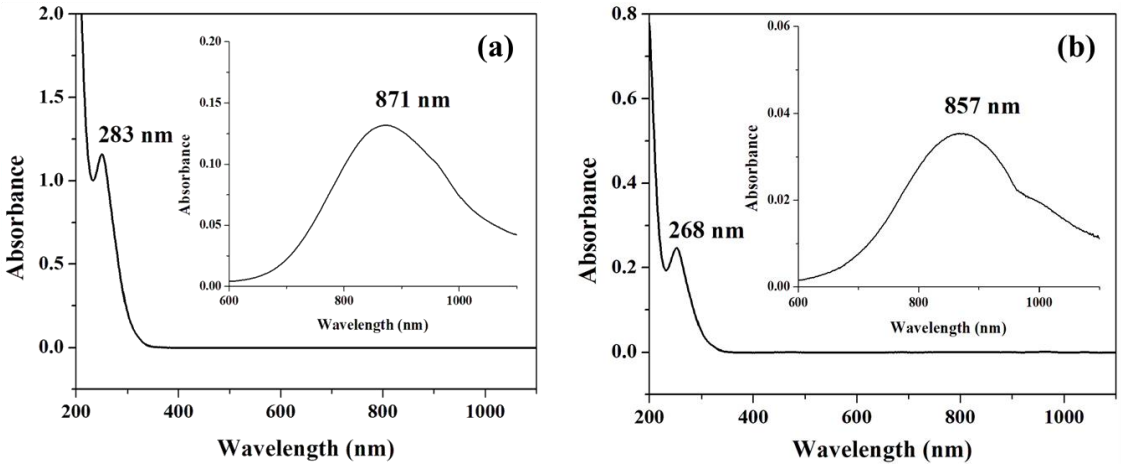

Figure 2. UV-Visible spectra of aqueous solutions of (a) $PW_{11}Cu$ and (b) $PW_{11}Cu$-Im

The UV-Visible spectra of $PW_{11}Cu$ and $PW_{11}Cu$-Im in aqueous medium are shown in Figure 2. The UV-Vis spectrum of $PW_{11}Cu$ shows characteristic peak for O→W charge transfer at 283 nm. A broad peak with λ_{max} at 871 nm indicates d-d transition for Cu(II) [12] while $PW_{11}Cu$-Im shows two peaks, at 268 and 857 nm respectively. The observed shift in λ_{max} values may be due to replacement of the aqua ligand by imidazole.

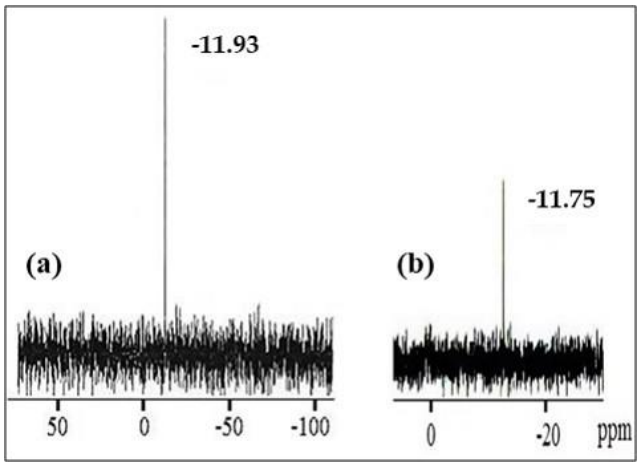

Figure 3. ^{31}P NMR Spectra of (a) $PW_{11}Cu$ and (b) $PW_{11}Cu$-Im

The ^{31}P NMR spectra of $PW_{11}Cu$ and $PW_{11}Cu$-Im are shown in figure 3. A single peak is observed at -11.75 ppm, indicating the formation of a single, pure product. No significant shift in the δ value of $PW_{11}Cu$-Im compared to $PW_{11}Cu$ (-11.93 ppm) suggests that the Keggin structure remains intact even after

functionalization. The slight downfield shift may be attributed to the changes in the environment around Cu and P due to transfer of electron density from Imidazole to the metal ion. Thus, ^{31}P NMR confirms that the aqua ligand in $PW_{11}Cu$ is replaced by Imidazole.

Table 2. ^{1}H NMR chemical shifts of Imidazole and $PW_{11}Cu$-Im

Functional group	Chemical Shift (ppm)	
	Imidazole	$PW_{11}Cu$-Im
C-H (single proton)	7.471	8.576
C-H (two equivalent protons)	6.846	7.55

Substitution of imidazole moiety can be confirmed from the ^{1}H NMR spectrum, shown in figure 4 as well as table 2. The proton NMR of imidazole is well known to have two peaks, a triplet of the single proton and a doublet of two equivalent protons with double the intensity of the triplet. The equivalence is seen despite the apparent difference of the two N atoms as the proton on N is very mobile and undergoes rapid exchange with either water or other imidazole molecules present, and is stabilized by resonance.

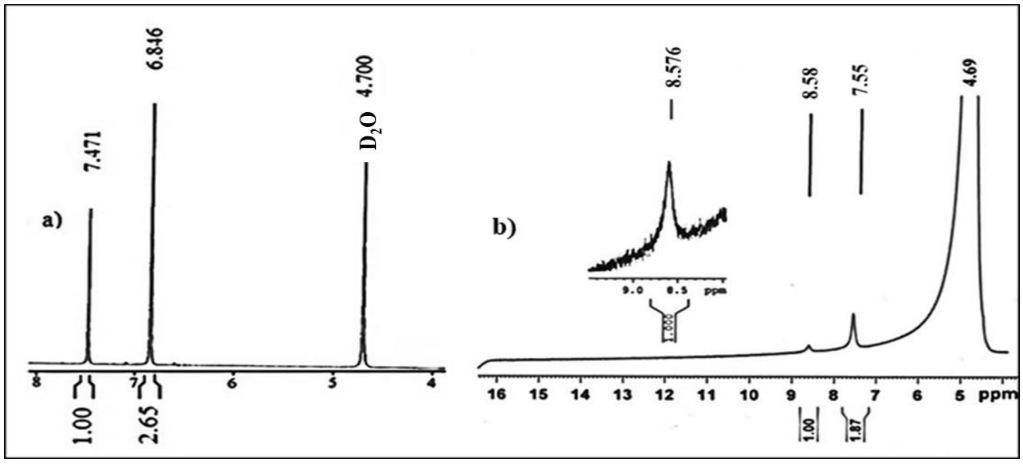

Figure 4. ^{1}H NMR spectra of (a) Imidazole and (b) $PW_{11}Cu$-Im

In the figure 4a, the peak at 7.471 ppm represents the single proton while that at 6.846 ppm represents the two equivalent protons. In case of $PW_{11}Cu$-Im (Figure

4b), a downfield shift and peak broadening are observed with the peaks at 8.576 and 7.55 ppm respectively. This may be due to the formation of N→Cu dative bond that results in the decrease in the electron density around the protons, making them more deshielded compared to the protons of pure imidazole.

Powder XRD patterns of (a) $PW_{11}Cu$ and (b) $PW_{11}Cu$-Im are shown in the figure 5. Powder XRD pattern of $PW_{11}Cu$ shows sharp peaks from 25 degrees to 35 degrees 2θ, which are characteristic of the Keggin structure in the complex. Sharp peaks at around 48 degrees 2θ also confirm the presence of copper in the lacuna of the Keggin structure.

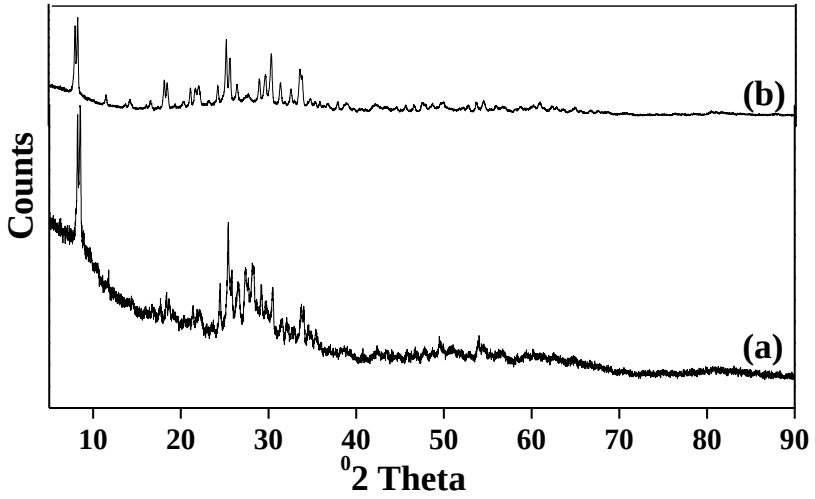

Figure 5. Powder XRD patterns of (a) $PW_{11}Cu$ and (b) $PW_{11}Cu$-Im

In case of $PW_{11}Cu$-Im, peaks corresponding to the Keggin structure remain intact confirming the retention of the structure. However, the observed drastic decrease in the intensity of the peaks corresponding to copper may be due to the presence of dative bond from N→Cu.

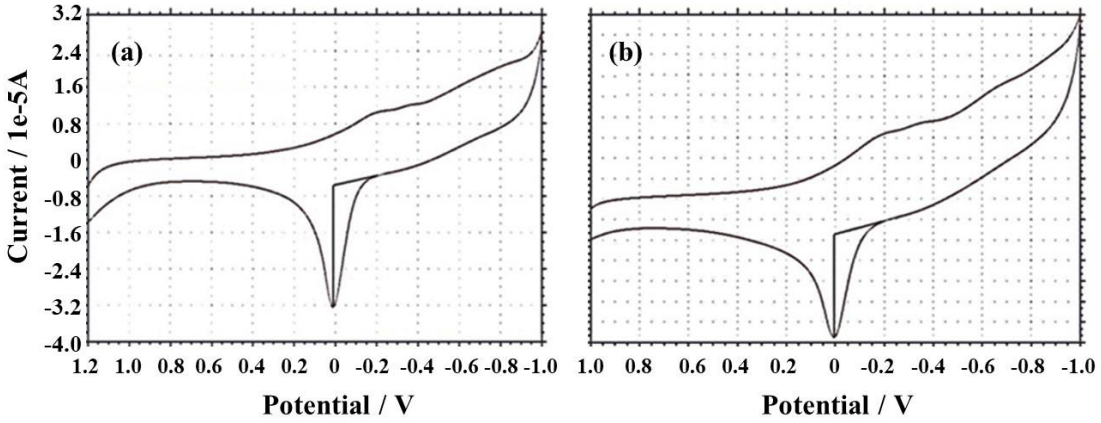

Figure 6. Cyclic Voltammograms of (a) $PW_{11}Cu$ and (b) $PW_{11}Cu$-Im

Cyclic Voltammetry of 1 mM solution of $PW_{11}Cu$-Im was recorded as described in chapter 1, and the voltammograms are presented in Figure 6. $PW_{11}Cu$ shows a quasireversible wave represented by anodic peak at 0.02V and cathodic peak at -0.2V indicating incorporation of Cu(II). Retention of the two peaks in $PW_{11}Cu$-Im along with a slight shift in the values indicates that Cu(II) is retained after functionalization.

Oxidation of styrene

A preliminary study using $PW_{11}Cu$-Im as the catalyst and H_2O_2 as the oxidant for the oxidation of styrene did not give a significant conversion. Thereafter, tert-butyl hydroperoxide (TBHP) was thought to be used as the oxidant. A detailed study was carried out for the oxidation of styrene using TBHP as oxidant and the reaction was optimized by varying various and the results are presented in Figure 7.

The effect of reaction time was assessed by varying the reaction time and keeping all other parameters constant (Figure 7a). With increase in time from 8 h to 10 h, there is increase in the conversion as well as selectivity of epoxide. However, when increased to 12 h, not much change in the conversion is observed, but the selectivity of styrene oxide reduces. Keeping into account the higher selectivity of styrene-oxide, 10 h was optimized.

The effect of amount of catalyst was evaluated (Figure 7b). When amount of catalyst was increased from 10 mg to 15 mg, substantial increase in conversion was seen. But further increase in catalyst amount results in decrease in conversion. This may be the result of blockage of catalytic sites. In all the cases, the selectivity remains more or less, constant. Hence, catalyst amount was optimized at 15 mg.

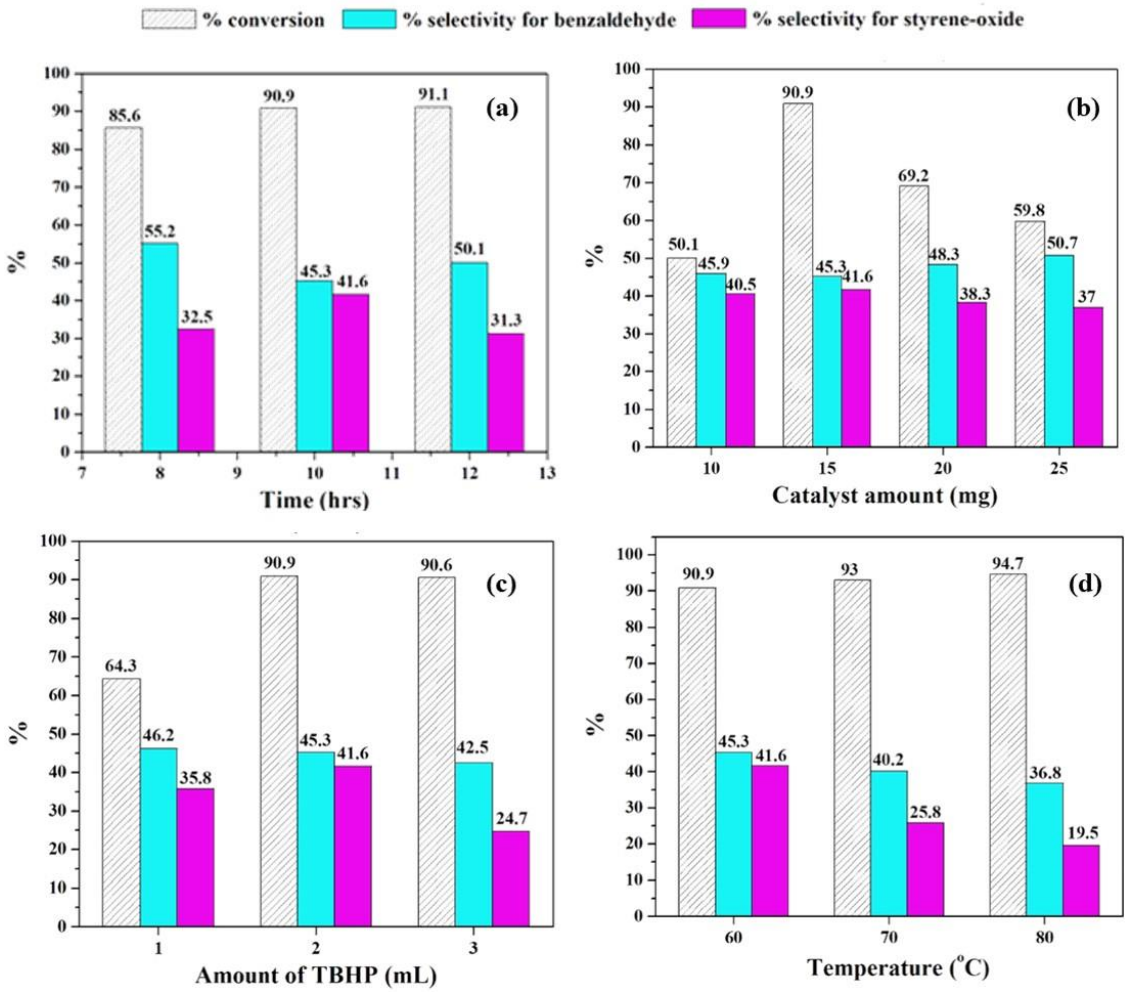

Figure 7. Optimization of parameters for oxidation of styrene (a) Effect of Time (Catalyst amount – 15 mg; temp – 60 ^{0}C; TBHP – 2 mL); (b) Effect of catalyst amount (Time – 10h; temp – 60 ^{0}C; TBHP – 2 mL); (c) Effect of amount of TBHP (catalyst amount – 15 mg; temp – 60 ^{0}C; time – 10h); (d) Effect of temperature (catalyst amount – 15 mg; time – 10h; TBHP – 2 mL)

As the amount of TBHP was varied from 1 mL to 2 mL, an increase in both, conversion and selectivity of epoxide was observed. But when increase further, though there was not much difference in conversion, the selectivity of epoxide decreased. Hence, the amount of TBHP was optimized at 2 mL (Figure 7c).

Effect of temperature was studies by increasing the temperature from 60 ^{0}C to 80 ^{0}C (Figure 7d). It was observed that with increase in temperature, there is not much change in conversion, but there is a significant decrease in selectivity of

the products as a result of degradation of TBHP. Hence, 60 ^{0}C was considered as optimum temperature.

The optimized conditions are as follows: Reaction time – 10 h; catalyst amount – 15 mg; amount of TBHP – 2 mL; reaction temperature – 60 ^{0}C. In the present case, like in previous cases, optimization of parameters have been carried out keeping into account the higher selectivity of styrene-oxide. But it must be noted that, depending upon the product requirement, the chemist can choose to vary the reaction conditions accordingly.

Oxidation of cis-cyclooctene

On similar lines, oxidation of cis-cyclooctene was carried out using the same catalyst and TBHP oxidant and the results are presented in figure 8.

Effect of amount of catalyst was studied and the catalyst amount was varied from 15 mg to 50 mg keeping all other parameters constant. From 15 mg to 25 mg, a significant increase in conversion was observed. Further increase in catalyst amount resulted in decrease in conversion, attributed to blocking of active sites. Hence, the catalyst amount was optimized at 25 mg.

The reaction was then set at different hours, in order to understand effect of reaction time on the catalytic activity. With increase in the time from 12 h to 20 h, there is a steady increase in the conversion of substrate. Further increase in time did not show significant increase in conversion. Thus, 20 h was considered as optimum time required for the reaction.

Amount of TBHP was varied and with increase in amount of TBHP from 1 mL to 1.5 mL, there is steady increase in conversion of cis-cyclooctene. But with further increase in amount of TBHP to 2 mL, there is a decrease in selectivity of epoxide with formation of unwanted products. Thus, 1.5 mL TBHP was considered optimum for the reaction.

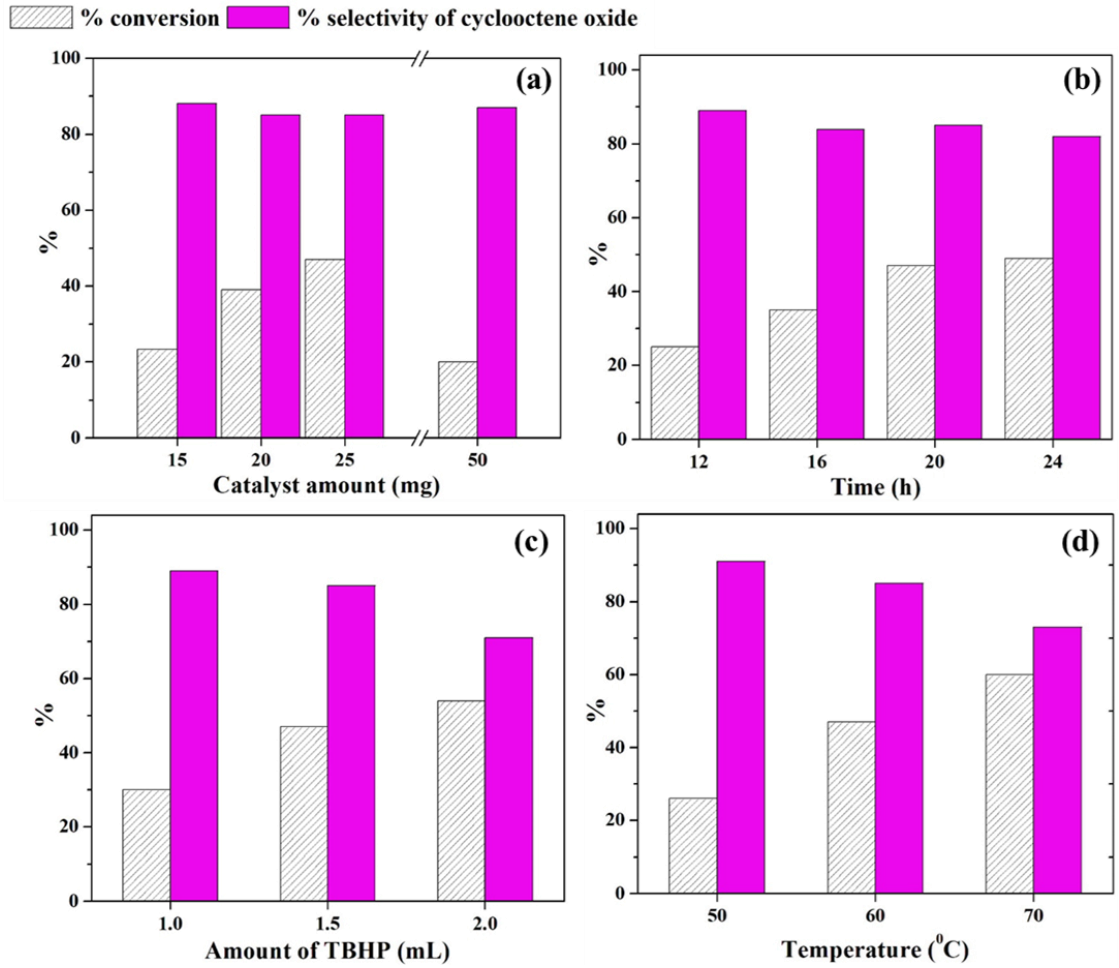

Figure 8. Optimization of parameters for oxidation of cis-cyclooctene (a) Effect of catalyst amount (Time–20 h; temp–60 ^{0}C; TBHP–1.5 mL); (b) Effect of time (Catalyst amount–25 mg; temp–60 ^{0}C; TBHP–1.5 mL); (c) Effect of amount of TBHP (catalyst amount–25 mg; temp–60 ^{0}C; time–20 h); (d) Effect of temperature (catalyst amount–25 mg; time–20 h; TBHP–1.5 mL)

Finally, the temperature was varied from 50 ^{0}C to 70 ^{0}C, which showed steady increase in conversion of cis-cyclooctene. But from 60 ^{0}C to 70 ^{0}C, the selectivity of epoxide decreases drastically, with formation of by-products. Hence 60 ^{0}C was considered optimum temperature.

Under optimized conditions, 47% conversion and 85% selectivity of cyclooctene-oxide were obtained. The optimized conditions are as follows: Catalyst amount – 25 mg; Time – 20 h; Amount of TBHP – 1.5 mL and Temperature – 60 ^{0}C.

Heterogeneity

The catalyst was tested to see if it truly is heterogeneous in nature following the procedure described in previous chapters. On analysis of the filtrate, it was seen that there was no significant change in the conversion and selectivity of the products, proving that the present catalyst was truly heterogeneous in nature. The results are presented in table 3.

Table 3. Test for Heterogeneity

Substrate	Reaction time	% conversion	% selectivity	
			Epoxide	Aldehyde/Ketone
Styrene [a]	5 h	51	33	41
	7 h (Filtrate)	51	33	40
Cis-cyclooctene [b]	16 h	35	84	16
	20 h (Filtrate)	36	85	15

[a] Catalyst amount – 15 mg; Time – 10 h; TBHP – 2 mL; Temp – 60 ^{0}C

[b] Catalyst amount – 25 mg; Time – 20 h; TBHP – 1.5 mL; Temp – 60 ^{0}C.

Control Experiments

In order to understand the effect of imidazole and also to affirm chemical interaction, experiments were carried out with $PW_{11}Cu$, Imidazole and physical mixture of $PW_{11}Cu$ + Im under the optimized conditions, and the results for both substrates are provided in table 4. In case of styrene, $PW_{11}Cu$-Im shows a drastic increase in conversion and selectivity of the products compared to that of $PW_{11}Cu$. The increase in the conversion may be due to synergic effect of $PW_{11}Cu$ and imidazole, while the increase towards the epoxide selectivity may be due to the presence of imidazole. Mizuno et al have explained that imidazole plays a dual role during the course of the reaction. The free nitrogen of the imidazole gets protonated, wherein the oxidant acts as the proton source. This initiates the oxidation of styrene. Secondly, as a Lewis base, imidazole suppresses the overall acidity of the catalyst, which inhibits the acid-catalyzed ring opening of

epoxides. As a result, there is higher selectivity towards the epoxide [13]. Functionalization of $PW_{11}Cu$ with Im generates a balance between the Lewis acidity and basicity of the catalyst, and thus high conversion and selectivity for epoxide is obtained. Similar results were obtained in case of cis-cyclooctene, wherein the functionalized material gave best conversion compared to the individual components, confirming the above explanation.

Table 4. Control Experiments

Catalyst	[i] Styrene oxidation % Conv. (Ald / Epo)	[ii] Cis-cyclooctene oxidation % Conv. (Epo / Ket)	Turn Over Number (i/ii)
$PW_{11}Cu$	35 (60 / 30)	25 (87 / 13)	841/349
Imidazole	42 (33 / 29)	16 (90 / 10)	974/226
$PW_{11}Cu$-Im	91 (45 / 42)	47 (85 / 15)	2185/676
$PW_{11}Cu$ + Im (Physical mix.)	58 (53 / 35)	33 (82 / 18)	-/-

i. Styrene oxidation. Active amount of Cu – 0.27 mg; Active amount of Imidazole – 0.29 mg; Time – 10 h; TBHP – 2 mL; Temp – 60 ^{0}C

ii. Cis-cyclooctene oxidation. Active amount of Cu – 0.45 mg; Active amount of Imidazole – 0.48 mg; Time – 20 h; TBHP – 1.5 mL; Temp – 60 ^{0}C

It is interesting to note that the physical mixture of $PW_{11}Cu$ + Im leads to a drastic decrease in conversion compared to $PW_{11}Cu$-Im for both substrates, confirming the attachment of two components via weak forces of interactions, which is already confirmed by FT-IR. Thus, catalytic study was used as a tool to explain the interactions between organic and inorganic component very well.

Kinetics

A detailed kinetic study was carried out for oxidation of styrene as well as cis-cyclooctene, as described in chapter 1.

An experiment was carried out with different concentrations of the substrates and TBHP, keeping catalyst concentration constant and the relationship between individual concentrations and time was obtained using equation 1 (Chapter 1). A plot of log[(b-x)/(a-x)] versus t (Figure 9) showed linear relationship in both the cases, which indicated that rate of reaction shows first order dependence on concentration of the substrates as well as TBHP, individually [14].

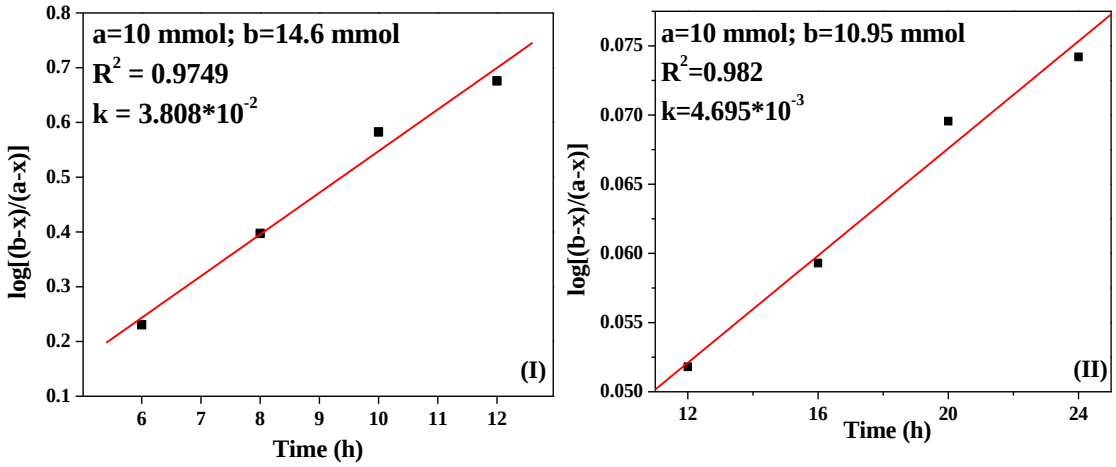

Figure 9. Plot of log[(b-x)/(a-x)] versus t for oxidation of (I) styrene and (II) cis-cyclooctene

A second experiment, with the same concentrations for the substrates and TBHP was carried out and a relationship was obtained between the concentration and time using equation 2 (Chapter 1).

Under two different initial concentrations of the reactants, the plot of 1/(a-x) versus t showed linearity (Figure 10) for styrene as well as cyclooctene, which indicated that rate of the reaction showed an overall second order dependence with respect to concentration of the substrates and TBHP [14].

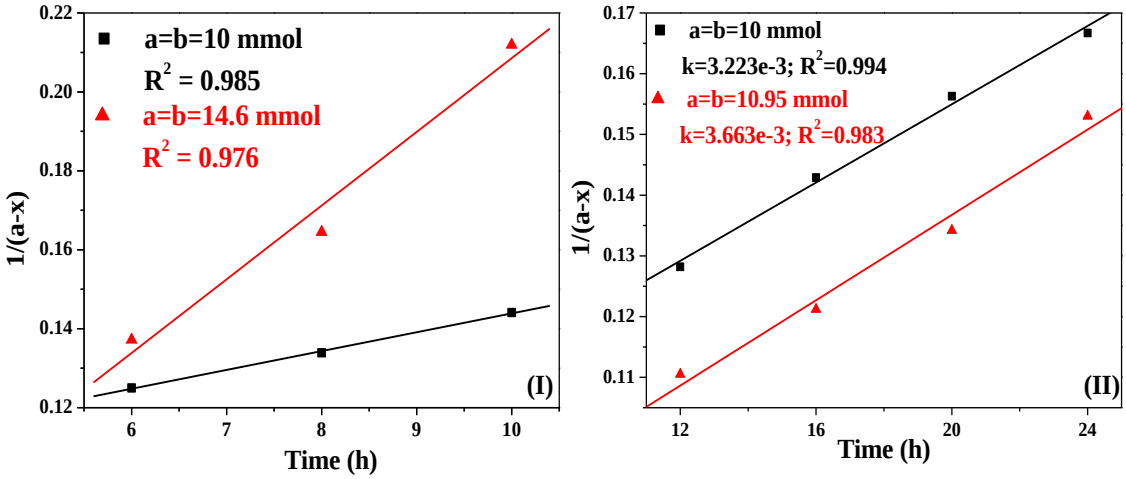

Figure 10. Plot of 1/(a-x) versus t for oxidation of (I) styrene and (II) cis-cyclooctene

Further, experiments with varied catalyst amounts were carried and a linear increase in rate constant (k) was obtained with increase in catalyst concentration in both the cases, indicating that reaction follows first order dependence with respect to the catalyst concentration also (Figure 11).

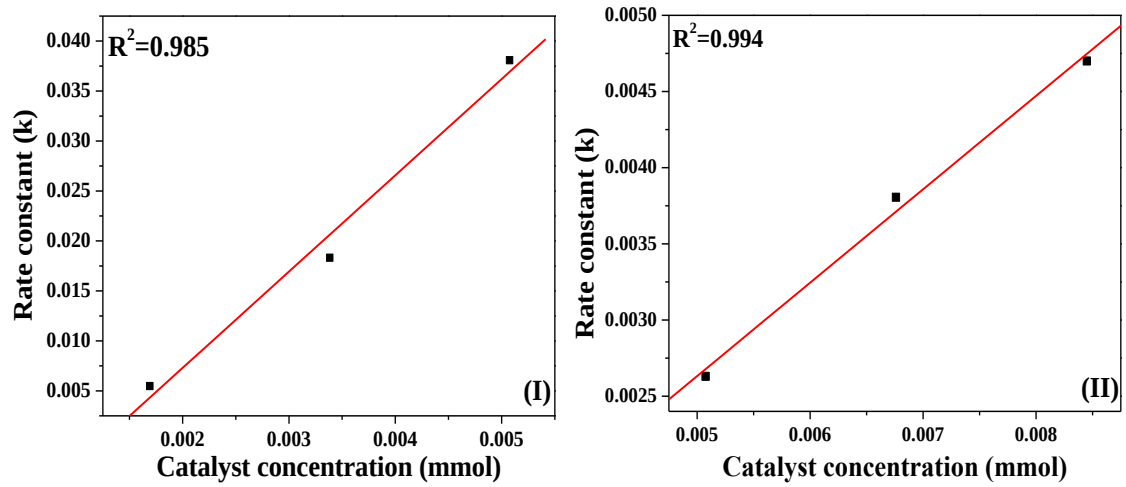

Figure 11. Plot of rate constant (k) versus catalyst concentration of (I) styrene and (II) cis-cyclooctene

Determination of Activation Energy

In order to understand the dependence of reaction rate on temperature, 1/T was plotted against lnk. Linearity was obtained for both the substrates (Figure 12), and the activation energy is obtained using Arrhenius's equation.

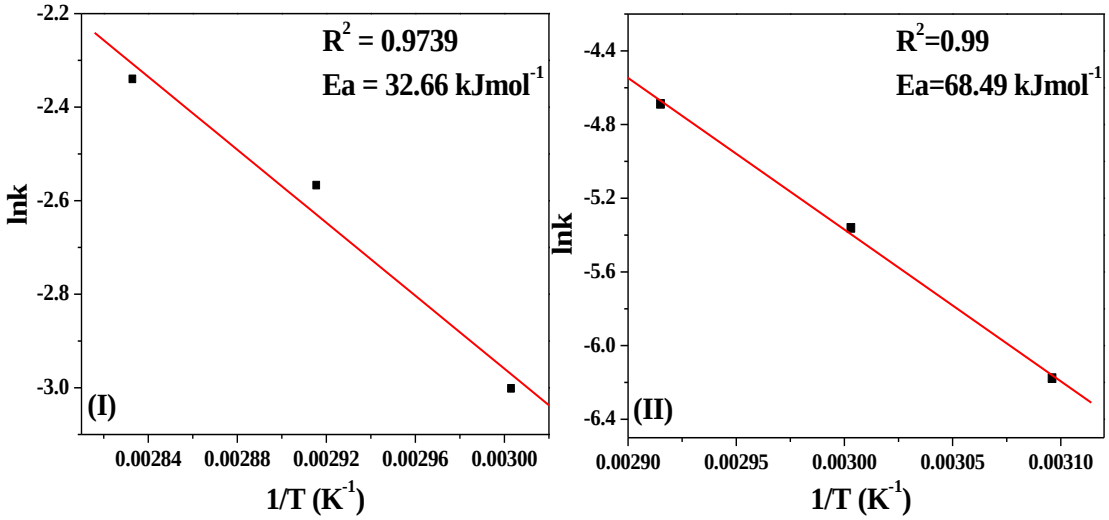

Figure 12. Plot for determination of activation energy of (I) styrene and (II) cis-cyclooctene

The Ea obtained was 32.66 kJmol^{-1} for styrene oxidation and 68.49 kJmol^{-1} for cyclooctene oxidation, which confirming that the reaction is governed by a truly chemical step, and the utilization of the catalyst takes place to maximum potential.

Mechanistic Investigation

Table 5. Inhibition Experiment with 2,6-di-tert-butyl-4-methylphenol as radical scavenger

Substrate	Reaction time	% conversion	% selectivity	
			Epoxide	Aldehyde/Ketone
Styrene [a]	8 h	86	32	55
	10 h	87	32	56
Cis-cyclooctene [b]	16 h	35	84	16
	20 h	36	83	17

[a] Catalyst amount - 15 mg; temp - 60 ^{0}C; TBHP - 2 mL

[b] Catalyst amount - 25 mg; temp - 60 ^{0}C; TBHP - 1.5 mL

Similar experiments to those in chapter 1, using radical scavenger were performed. No significant change in conversion and selectivity after addition of

the scavenger for styrene as well as cis-cyclooctene, confirmed that a radical intermediate is formed and the reaction proceeds by radical mechanism (Table 5).

Recycle study

The catalyst was recycled following similar procedure as described in chapter 1 and was then used for oxidation under optimized conditions. Negligible changes in conversion and selectivity of the products for both reactions confirmed that the hybrid catalyst remained stable during the reaction and can be reused for multiple cycles (Table 6).

Table 6. Recycle study

Catalyst	% conversion	% selectivity	
		Epoxide	Aldehyde/Ketone
$PW_{11}Cu$-Im	[a]91/[b]47	[a]42/[b]85	[a]45/ [b]15
R_1-$PW_{11}Cu$-Im	[a]90/ [b]47	[a]40/ [b]84	[a]46/ [b]16
R_2-$PW_{11}Cu$-Im	[a]90/ [b]46	[a]41/ [b]85	[a]46/ [b]15
R_3-$PW_{11}Cu$-Im	[a]89/ [b]45	[a]40/ [b]85	[a]46/[b]15

[a] **Styrene oxidation.** Catalyst amount – 15 mg; TBHP – 2 mL; Time – 10 h; Temp – 60 ^{0}C

[a] **Cis-cyclooctene oxidation.** Catalyst amount– 25 mg; TBHP – 1.5 mL; Time – 20 h; Temp – 60 ^{0}C

Characterization of regenerated catalyst

The regenerated catalyst was characterized using FT-IR and powder XRD. The FT-IR data of the fresh and regenerated catalysts are shown in the table 7. It can be seen that all the characteristic bands are retained in the regenerated catalyst.

Table 7. FT-IR frequencies of fresh and recycled catalysts

Catalyst	FT-IR bands (cm^{-1})								
	P-O	**W=O**	**W-O-W**	**Cu-O**	**Cu-N**	**C-H**	**C-C**	**N-H**	**C-N**
$PW_{11}Cu$-Im	1101 1068	962	883 810	-	435	3142 2900	1606	-	1490 1400 1310
Rec. $PW_{11}Cu$-Im	1101 1068	952	887 813	-	418	3142	1606	-	1508 1425 1308

This indicates that $PW_{11}Cu$-Im does not degrade during the course of the reaction and the structural morphology remains intact. It also shows that there is no leaching of either the Cu(II) centre or the imidazole moiety.

The wide angle powder XRD spectra of fresh and recycled catalyst are shown in figure 13. It can be clearly noted that the characteristic peaks of the Keggin anion between 25-35 degrees 2 Theta are retained in the recycled catalyst, indicating that the Keggin structure remains intact even after the catalyst is regenerated.

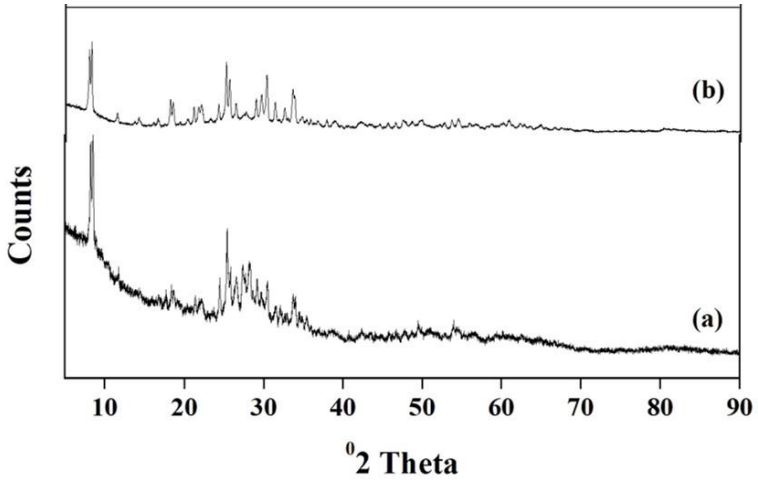

Figure 13. Powder XRD patterns of (a) Fresh and (b) recycled PW_{11}Cu-Im

Comparison of substrates

Table 8. Comparison of substrates

Substrate	% conversion	% selectivity		Activation energy (Ea, kJ/mol)
		Epoxide	Aldehyde/ Ketone	
Styrene	91	42	45	32.66
Cis-cyclooctene	10	93	7	82.18

[a] Catalyst amount: 15 mg; Time: 12h; temp: 60 ^{0}C; TBHP: 2 mL

A comparison of substrates (Table 8) shows that styrene shows much better catalytic activity than cis-cyclooctene and also under milder conditions, like in the previous cases. This is attributed to the morphology of the substrates, which, in case of styrene, is planar, while in case of cis-cyclooctene is non-planar. Also, the rigidity and bulkiness of the cyclic alkene does not allow easy oxidation of the double bond.

Summary

- $PW_{11}Cu$ was successfully functionalized with imidazole by ligand substitution technique and characterized in detail
- Spectral studies confirmed intact Keggin structure as well as formation of N→Cu dative bond.
- Catalytic evaluation and kinetic studies showed considerable increase in conversion and selectivity of epoxide compared to unfunctionalized complex at considerably lower Ea.
- Control experiments confirmed that this was due to synergic effect between inorganic and organic moieties.
- The catalyst recycled and reused up to three cycles without any loss in activity, and characterization of regenerated catalyst confirmed retention of structure.

References

[1] L. Han, P.-P. Zhang, H.-S. Liu, H.-J. Pang, Y. Chen and J. Peng, J. Cluster Sci., 81-91, (2010).

[2] C. Dablemont, A. Proust, R. Thouvenot, C. Afonso, F. Fournier and J.-C. Tabet, Inorg. Chem., 11, 3514-3520, (2004).

[3] H. Liu, C. J. Gómez-García, J. Peng, J. Sha, Y. Li and Y. Yan, Dalton Trans., 44, 6211-6218, (2008).

[4] P.-P. Zhang, J. Peng, J.-Q. Sha, A.-X. Tian, H.-J. Pang, Y. Chen and M. Zhu, CrystEngComm, 5, 902-908, (2009).

[5] X. Wang, J. Li, H. Lin, G. Liu, A. Tian, H. Hu, X. Liu and Z. Kang, J. Mol. Struct., 1, 99-103, (2010).

[6] Z. Nadealian, V. Mirkhani, B. Yadollahi, M. Moghadam, S. Tangestaninejad and I. Mohammadpoor-Baltork, J. Coord. Chem., 6, 1071-1081, (2012).

[7] B. Yuan, W. Zhao, F. Yu and C. Xie, Catal. Commun., 89-93, (2014).

[8] H.-F. Hao, W.-Z. Zhou, H.-Y. Zang, H.-Q. Tan, Y.-F. Qi, Y.-H. Wang and Y.-G. Li, Chemistry – An Asian Journal, 8, 1676-1683, (2015).

[9] A. Patel, J. Mater. Sci., 8, 4689-4699, (2016).

[10] R. Ramasamy, Armen. J. Phys., 51-55, (2015).

[11] K. Nakamoto and P. J. McCarthy, *Spectroscopy and structure of metal chelate compounds*, Wiley, (1968).

[12] C. Pichon, P. Mialane, A. Dolbecq, J. Marrot, E. Rivière, B. Keita, L. Nadjo and F. Sécheresse, Inorg. Chem., 13, 5292-5301, (2007).

[13] K. Kamata, K. Sugahara, R. Ishimoto, S. Nojima, M. Okazaki, T. Matsumoto and N. Mizuno, ChemCatChem, 8, 2327-2332, (2014).

[14] Y. Liang, C. Yi, S. Tricard, J. Fang, J. Zhao and W. Shen, RSC Adv., 23, 17993-17999, (2015).

Chapter 4B

(S)-1-Phenylethylamine functionalized mono-copper substituted phosphotungstate

Synthesis, Characterization and Catalytic Evaluation

As mentioned in the introduction, POMs present innumerable applications in the field of catalysis [1-8]. On the other hand, chirality is that remarkable phenomenon found in daily life, which has shown significance in pharmaceutical and chemical industry [9]. In an attempt to blend the advantages of POMs with the importance of chirality, remarkable endeavors have gone into development of chiral-POMs, such that, chiral-POM based materials as candidates for asymmetric catalysis and molecular recognition experiments have garnered interest of researchers in recent years [10, 11]. Indeed, chiral-POM hybrids play an important role of tuning the selectivity of the chiral product in such a way that high *enantiomeric excess* is obtained.

Chirality can be induced into a POM in two different ways. (1) They can be intrinsically chiral due to bond length alteration, geometric distortion, formation of structural lacunae or introduction of chiral metal frameworks. The drawbacks of these enantiomers are that POMs in acidic solutions are highly unstable, easily hydrolyze and racemize rapidly to lose their optical activity. (2) By introducing steriogenic side-chains in the form of chiral organic ligands by means of coordination bonding, electrostatic interactions and covalent modifications [12]. The advantages of this technique are that chirality is transferred from organic ligand to the symmetric POM, and also the new material possesses unusual characteristics. Therefore, this is the most common technique to synthesize chiral-POMs [13]. Many reviews, especially focusing on the synthesis and designing involving the second approach, are available on chiral-POM based materials [14-23].

Despite the diversity in chiral-POM based materials, those based specifically on transition metal substituted phosphotungstates are sparse. In 2005, Pope et al synthesized two Co-ethylene diamine (*en*) incorporated polyoxometalates, $Na_{6.5}K_{5.5}[K\subset\{Co(en)WO_4\}WO(H_2O)(PW_9O_{34})_2]\cdot 19H_2O$ and $Na_7K_5[\{Co(en)(\mu\text{-}OH)_2Co(en)\}\{PW_{10}O_{37}Co(en)\}_2]\cdot 20H_2O$, using coordination competition approach. These complexes were the first examples of polyoxometalates that

incorporate *embedded* chelated heteroatoms, which open a broad range of new steric and chiral possibilities for POMs. Of the two, the former shows mirror symmetry because of the fluxional behavior of *en* ligand, despite an overall C_1 symmetry. On the other hand, in the second complex, $[PW_{10}O_{37}Co(en)]^{6-}$ is chiral in nature and functions as a bidentate ligand between two Co(*en*) groups [24].

In 2012, Patel et al synthesized two chiral inorganic-organic hybrid molecules, by functionalizing mono-Mn substituted phosphotungstate with S-(+)-sec-butyl amine and R-(-)-1-cyclohexyl ethylamine by ligand substitution approach and described their detailed characterization [25, 26]. More recently, the same group reported synthesis of a mono-ruthenium substituted phosphotungstate functionalized with R-(-)-1-cyclohexyl ethylamine using the same approach, and its catalytic activity for the aerobic asymmetric oxidation of styrene [27].

A literature survey shows that mono-copper substituted phosphotungstate has never been functionalized using chiral organic ligand. In an attempt to execute the same, here we have functionalized $PW_{11}Cu$ using a simple chiral molecule, and (*S*)-1-Phenylethylamine (*S*-PEA) was chosen as a model ligand. The synthesized material was characterized by various techniques and then evaluated for its catalytic activity for asymmetric oxidation of styrene. Studies were also carried out using different green oxidants with an effort to obtain maximum *enantiomeric excess* (*ee*) of the chiral product.

EXPERIMENTAL

Materials.

All chemicals used were of A.R. grade. 12-tungstophosphoric acid, Copper chloride dihydrate, Cesium chloride, Sodium hydroxide, Styrene, 70% TBHP and Dichloromethane were obtained from Merck. *S*-PEA was obtained from TCI Chemicals, Chennai, while $NaHCO_3$ was obtained from SRL, Mumbai. All chemicals were used as received.

Synthesis of hybrid material was carried out in two steps.

I. Synthesis of mono-copper substituted phosphotungstate ($PW_{11}Cu$)

$PW_{11}Cu$ was synthesized by the one-pot method mentioned in chapter 1.

II. Functionalization of $PW_{11}Cu$ with S-(+)-1-phenyl ethylamine

0.35g (0.1 mmol) of $PW_{11}Cu$ was dissolved in 10 mL water by heating. 50 µL (0.1 mmol) of *S*-PEA was dissolved 10 mL methanol. The methanolic solution of S-PEA was added drop-wise to the hot, clear solution of $PW_{11}Cu$ while stirring. The pH was adjusted to 6.4 using dil. NaOH. The resultant mixture was refluxed for 24 h at 90 ^{0}C, cooled, filtered and dried at 100 ^{0}C. The obtained light green powder was designated as $PW_{11}Cu$-*S*-PEA (Scheme 1).

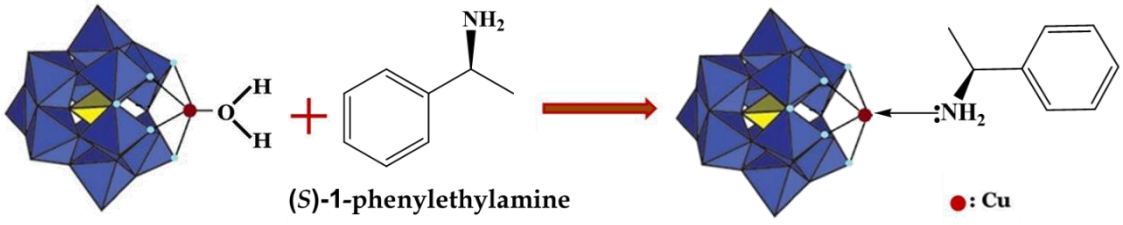

Scheme 1. Functionalization of $PW_{11}Cu$ with *S*-PEA

Catalytic reaction

Oxidation of the styrene was carried out using $PW_{11}Cu$-*S*-PEA as catalyst, following the method mentioned in chapter 1. Oxidation of cis-cyclooctene was not carried out as there are no chiral products to be formed.

RESULTS AND DISCUSSION

Catalyst Characterization

Elemental Analysis of $PW_{11}Cu$-*S*-PEA was carried out using ICP-AES as well as EDX and the obtained results were in good agreement with the theoretical ones. Theoretical: P, 0.87; W, 57.05; Cu, 1.79; C, 2.71; N, 0.40. Experimental: P, 0.76; W, 56.65; Cu, 1.81; C, 2.91; N, 0.51.

TGA of *S*-PEA shows 99.2% weight loss up to 150 ^{0}C. TGA of $PW_{11}Cu$-*S*-PEA (Figure 1) shows an initial weight loss of 1.8% up to 120 ^{0}C attributed to loss of adsorbed water as well as partial decomposition of the organic ligand. Further weight loss of 1.7 % up to 370 ^{0}C is attributed to complete decomposition of *S*-PEA. The total number of water molecules was calculated and found to be 1. From elemental as well as TGA, the molecular formula of the synthesized material is $Cs_5[PW_{11}O_{39}Cu(C_8H_{11}N)].H_2O$

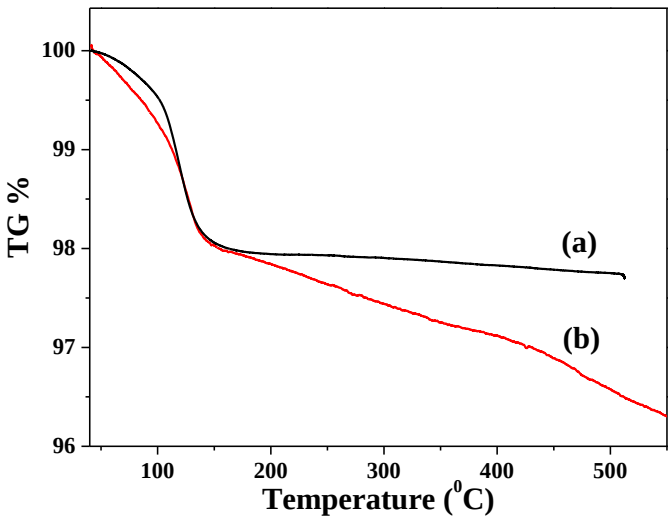

Figure 1. TGA of (a) $PW_{11}Cu$ and (b) $PW_{11}Cu$-*S*-PEA

Figure 2 shows FT-IR spectra of (a) $PW_{11}Cu$ (b) $PW_{11}Cu$-*S*-PEA and (c) *S*-PEA. The FI-IR spectra of $PW_{11}Cu$ has already been discussed in chapter 1. The FT-IR spectra of pure *S*-PEA shows characteristic bands of –NH str. vibrations at 3433 cm^{-1}, aromatic ring str. at 3062 and 3032 cm^{-1}, methyl str. at 2924 cm^{-1} and C=C str. at 1490 and 1450 cm^{-1}. The FT-IR spectrum of $PW_{11}Cu$-*S*-PEA shows bands of both, $PW_{11}Cu$ and *S*-PEA, but with a slight shift in all bands, indicating functionalization of the POM with organic ligand. Along with this, an additional band is observed at 516 cm^{-1}, attributed to Cu-N stretching vibrations.

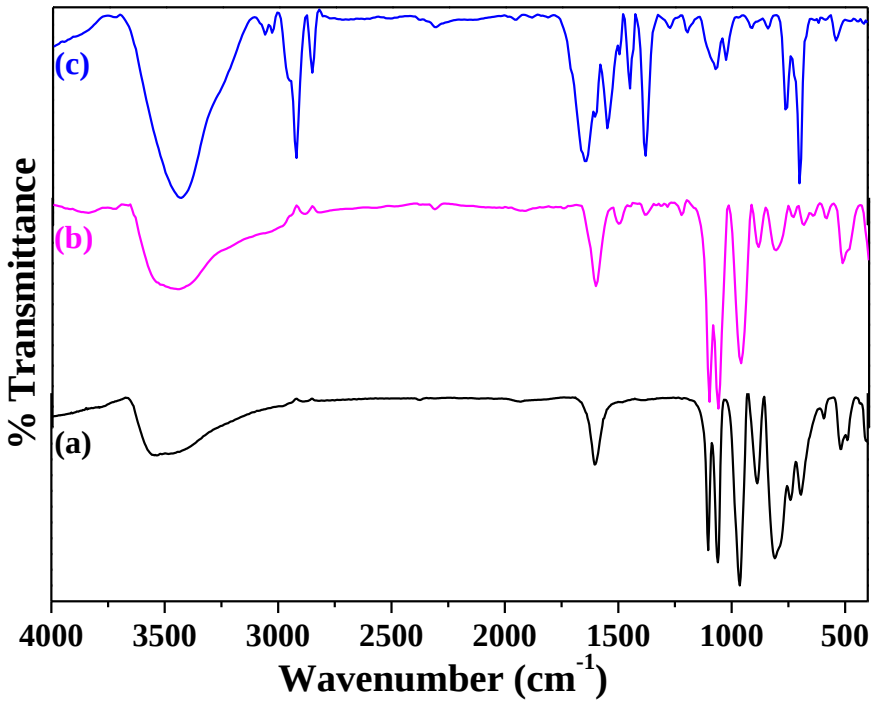

Figure 2. FT-IR spectra of (a) $PW_{11}Cu$ (b) $PW_{11}Cu$-*S*-PEA and (c) *S*-PEA

Due to the solubility problem of the present material, we could not perform the solution NMR, and hence, solid state NMR was carried out. This is the reason for not getting sharp NMR peaks. The ^{31}P MAS NMR of $PW_{11}Cu$-*S*-PEA did not show any peak, which may be because the core of the POM unit, where phosphorus atom is present, is heavily shielded by the organic ligand. However, substitution of the chiral ligand has been confirmed by ^{13}C MAS NMR. The spectra is presented in figure 3, while chemical shifts values of pure and functionalized *S*-PEA are shown in table 1. The ^{13}C MAS NMR of *S*-PEA shows

characteristic peaks at 126.9, 128.5 and 147.9 ppm corresponding to aromatic carbons, 25.6 ppm corresponding to methyl carbon and 51.3 ppm corresponding to chiral carbon respectively.

Table 1. ^{13}C MAS NMR chemical shifts of S-PEA and $PW_{11}Cu$-S-PEA

Functional group		Chemical Shift (ppm)	
		***S*-PEA**	**$PW_{11}Cu$-*S*-PEA**
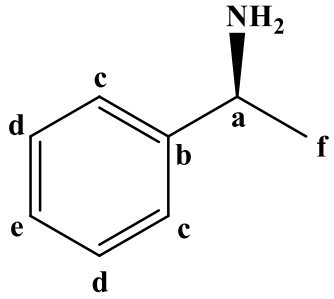	A	51.3	74.9
	B	147.9	105.8
	C	126.9	88.8
	D	128.5	
	E	126.7	
	F	25.6	66.4

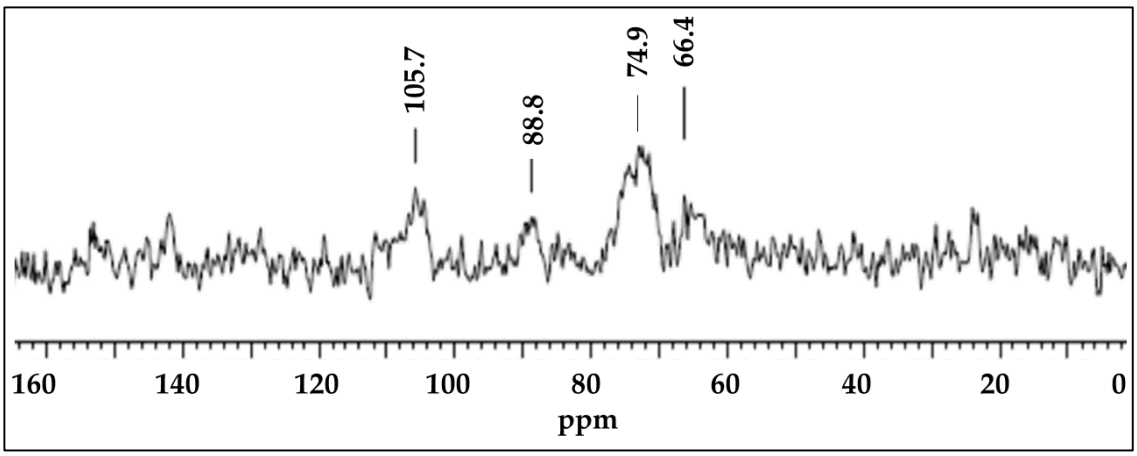

Figure 3. ^{13}C MAS NMR spectra of $PW_{11}Cu$-*S*-PEA

NMR spectra of $PW_{11}Cu$-*S*-PEA also shows all the characteristic peaks with shifting, indicating the intact structure of ligand as well as successful functionalization. The chiral carbon shows further downfield shift from 51.3 ppm to 74.9 ppm. Similarly, the chemical shift of the methyl carbon also is highly deshielded, giving peak at 66.4 ppm. The drastic shift of δ values towards downfield region is attributed to loss of electronegativity around the adjacent

nitrogen. This indicates that the lone pair of electrons is used up for the formation of N→Cu dative bond. On the other hand, the aromatic carbons display an upfield shift is, and this may be because of the electron rich POM unit, that shields the aromatic carbons.

The ESR spectra of $PW_{11}Cu$ and $PW_{11}Cu$-S-PEA are shown in figure 4. As described in chapter 1, $PW_{11}Cu$ gives a five-line hyperfine spectrum characteristic of Cu(II) in octahedral or distorted octahedral geometry. $PW_{11}Cu$-S-PEA shows a similar spectrum indicating that copper exists in +2 state even after functionalization and that the geometry is retained. The decrease in the intensity of the hyperfine lines may be attributed to interactions of Cu centre with the ligand, as expected.

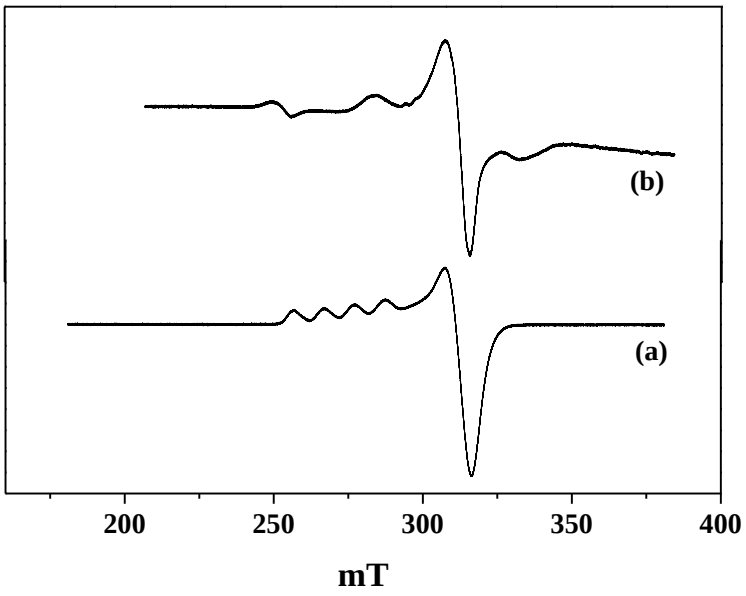

Figure 4. LNT ESR spectra of (a) $PW_{11}Cu$ and (b) $PW_{11}Cu$-S-PEA

Wide angle powder XRD spectra of $PW_{11}Cu$ and $PW_{11}Cu$-*S*-PEA are shown in figure 5. The powder XRD pattern of $PW_{11}Cu$-S-PEA is similar to that of unfunctionalized $PW_{11}Cu$, indicating the intact structure of Keggin unit. Further, slight shift in the 2θ value of copper and also the decrease in intensity of peaks in case of $PW_{11}Cu$-*S*-PEA may be because of chemical interaction between N and Cu.

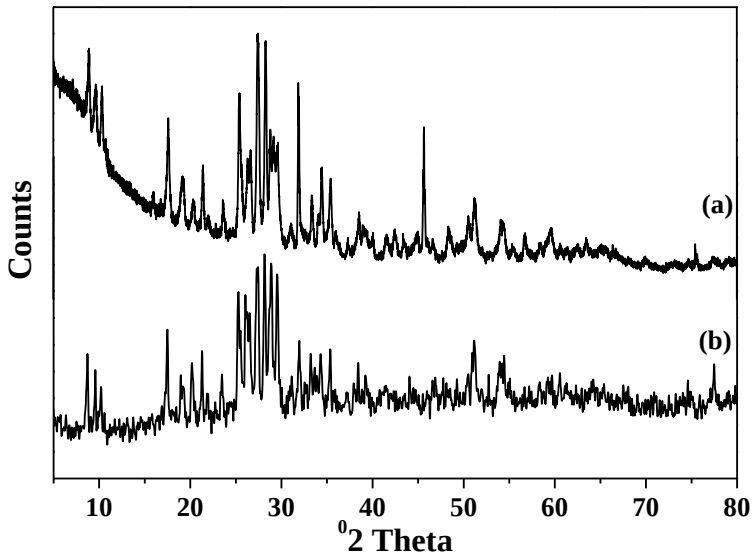

Figure 5. Powder XRD spectra of (a) $PW_{11}Cu$ and (b) $PW_{11}Cu$-*S*-PEA

Optical Rotation

In order to study the chirality of the synthesized material, optical rotation studies were carried out using pulse polarimeter. A stock solution containing 5 mg of $PW_{11}Cu$-*S*-PEA in 10 mL double distilled water was prepared. After a blank run using distilled water, the stock solution was placed in the sample holder and the relative optical rotation was recorded. While the pure ligand showed optical rotation ranging from α 20/D -37– -41^0, the synthesized material gave a relative optical rotation value of -0.7471^0. This confirmed that the synthesized material showed chirality, but the very small value compared to pure ligand was attributed to two reasons (a) sparingly soluble nature of material and (b) the concentration of the chiral ligand in the synthesized material is very less (~4 wt%). The presence of chirality if further confirmed by CD spectroscopy.

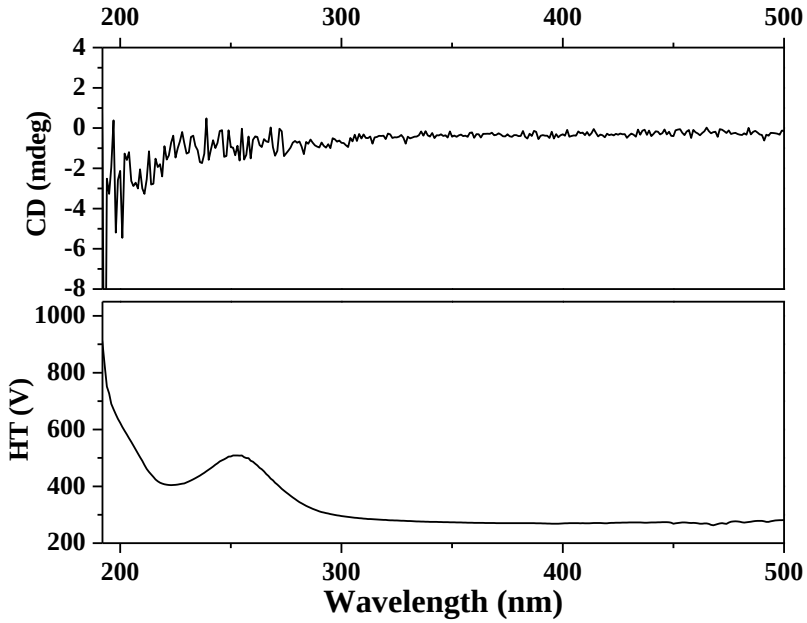

Figure 6. CD spectra of $PW_{11}Cu$-S-PEA

The CD spectra of $PW_{11}Cu$-S-PEA (Figure 6) indicates that optical rotation activity has been induced in the POM moiety, due to chemical interaction with the chiral ligand, confirming the observations of polarimetry experiment. The intensity of the induced chirality seem to be very less, which may be because of the concentration of chiral ligand as well as solubility of the synthesized complex, as explained previously. Further, the functionalized material exhibits strong Cotton effect at around 250 nm, which is the fingerprint region for O → W charge transfer in Keggin structures [28].

Asymmetric oxidation of styrene

Oxidation of styrene was carried out using TBHP as the oxidant and various parameters were optimized with an aim to obtain maximum *enantiomeric excess*. The reaction was carried out at different catalyst amounts and from 10 mg to 20 mg (Figure 7), steady increase in conversion as well as selectivity of styrene oxide is observed. As expected higher selectivity of the *S*- isomer is obtained, but maximum *ee* of only 4 was attained. From the results obtained, 20 mg catalyst was considered optimum.

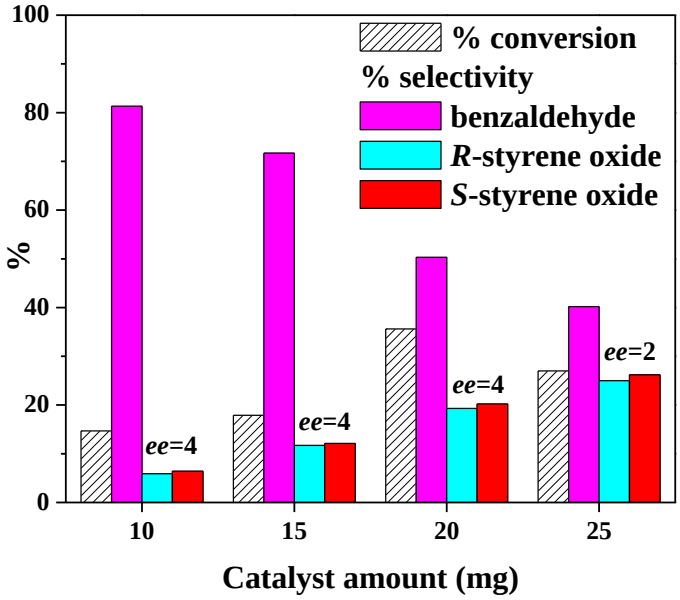

Figure 7. Effect of Catalyst amount (Time – 16 h; temp – 60 ^{0}C; TBHP – 2 mL)

Next, when the reaction time is varied from 8 h to 12 h, there is an increase in conversion and selectivity of epoxide along with its *ee* (Figure 8). With further increase in reaction time, no increase in conversion was observed, but the selectivity as well as the *ee* of *S*- isomer of epoxide reduced. Hence, 12 h was considered optimum time for the reaction.

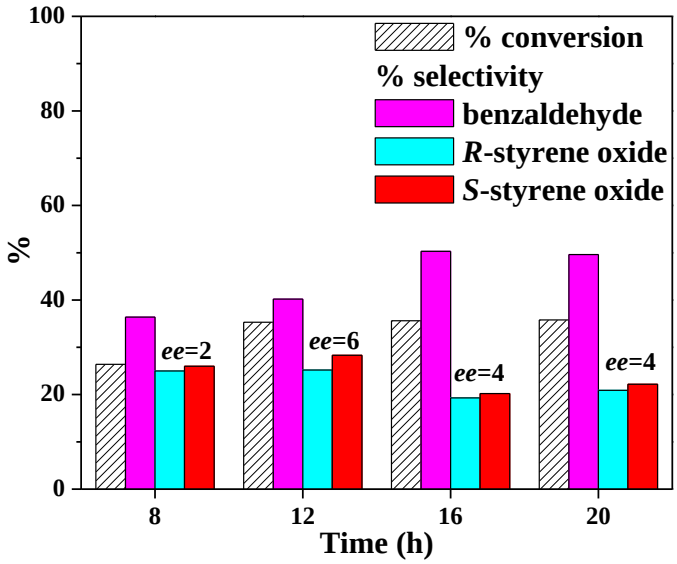

Figure 8. Effect of Time (Catalyst amount – 20 mg; temp – 60 ^{0}C; TBHP – 2 mL)

With a view to obtain better *ee*, the reaction was carried out using different green oxidants, and the results are presented in table 2. The reactions using H_2O_2 and molecular O_2 were carried out at 80 ^{0}C, while a few drops of TBHP (~0.2 mL) was added as an initiator in case of molecular O_2. It is interesting to note that despite lower selectivity of the epoxide, reaction with molecular O_2 gave higher *ee* of 16. This can be explained as follows.

Table 2. Effect of oxidants

Oxidant	% conversion	% selectivity			*ee*
		Benzaldehyde	*R*-styrene oxide	*S*-styrene oxide	
[a] **TBHP**	36	63	21		-
[b] **TBHP**	35	40	25	28	6
[c] **H_2O_2**	N.A.	-	-	-	-
[d] **O_2**	43	63	13	18	16

[a] Without catalyst; Time – 12 h; TBHP – 2 mL; Temp – 60 ^{0}C

[b] Catalyst amount – 20 mg, Time – 12 h; TBHP – 2 mL; Temp – 60 ^{0}C

[c] Catalyst amount – 20 mg, Time – 12 h; Styrene:H_2O_2 – 1:3; Temp – 80 ^{0}C

[d] Catalyst amount – 20 mg, Time – 12 h; Styrene – 100 mmol; TBHP – 0.2 mL; Temp – 80 ^{0}C

As mentioned in chapter 1, TBHP tends to undergo self-disproportionation in the absence of catalyst. Hence, reaction in the absence of catalyst gives low selectivity for epoxide, as a racemic mixture (Table 2, entry 1). On the other hand, TBHP with chiral catalyst shows similar conversion, but the epoxide is no longer racemic (*ee* = 6). Here, it can be assumed that majority of the TBHP molecules undergo self-disproportionation, while a small number of molecules interact with the catalyst, thereby giving a small *ee*. In the case of molecular oxygen, self-disproportionation does not occur, and hence entire oxidant has to interact with the catalyst to form intermediate which leads to formation of epoxide with high value of *ee*.

Further detailed studies was not carried out with molecular oxygen, as the entire thesis deals with use of TBHP as oxidant.

Summary

- $PW_{11}Cu$ was successfully functionalized with chiral organic ligand, S-(-)-1-phenylethylamine by ligand substitution approach and thoroughly characterized.
- FT-IR and ^{13}C MAS NMR confirmed the formation of N→Cu dative bond, while optical rotation studies and CD spectroscopy affirmed the chirality of the material.
- The material was evaluated for its activity for asymmetric oxidation of styrene, and vith a view to obtain high *ee*, different oxidants were used.
- While TBHP gave high selectivity for epoxide, the best *ee* was obtained with molecular oxygen. This is attributed to the inability of oxygen to undergo self-disproportionation, as a result of which, it forms the reactive intermediate with the chiral catalyst to give high enantioselectivity.

Reference

[1] M. Pope and A. Muller, *Polyoxometalates: From Platonic Solids to Anti-Retroviral Activity: From Platonic Solids to Anti-Retroviral Activity*, Springer Netherlands, (1994).

[2] Issue on Polyoxometalates, Chem. Rev., 1, 1-390, (1998).

[3] K. Y. Lee and M. Misono, *Handbook of Heterogeneous Catalysis*, 2, (G. Ertl, H. Knözinger, F. Schüth and J. Weitkamp) Wiley-VCH, (2008).

[4] C. L. Hill, J. Mol. Catal. A: Chem., 1-2, 1-242, (2007).

[5] N. Mizuno, S. Hikichi, K. Yamaguchi, S. Uchida, Y. Nakagawa, K. Uehara and K. Kamata, Catal. Today, 1, 32-36, (2006).

[6] I. V. Kozhevinikov, *Polyoxometalate Molecular Science*, (J. J. Borrás-Almenar, E. Coronado, A. Müller and M. Pope) Springer Netherlands, (2003).

[7] R. Neumann, *Polyoxometalate Molecular Science*, (J. J. Borrás-Almenar, E. Coronado, A. Müller and M. Pope) Springer Netherlands, (2003).

[8] C. Boglio, K. Micoine, P. Rémy, B. Hasenknopf, S. Thorimbert, E. Lacôte, M. Malacria, C. Afonso and J.-C. Tabet, Chem. Eur. J., 19, 5426-5432, (2007).

[9] Berichte der Bunsengesellschaft für physikalische Chemie, 1, 96-96, (1995).

[10] B. Hasenknopf, K. Micoine, E. Lacôte, S. Thorimbert, M. Malacria and R. Thouvenot, Eur. J. Inorg. Chem., 32, 5001-5013, (2008).

[11] D.-Y. Du, L.-K. Yan, Z.-M. Su, S.-L. Li, Y.-Q. Lan and E.-B. Wang, Coord. Chem. Rev., 3, 702-717, (2013).

[12] J. Zhang, Y. Huang and Y. J. T. i. P. R. Wei, 37, (2015).

[13] W.-L. Chen, H.-Q. Tan and E.-B. Wang, J. Coord. Chem., 1, 1-18, (2012).

[14] A. Proust, B. Matt, R. Villanneau, G. Guillemot, P. Gouzerh and G. Izzet, Chem. Soc. Rev., 22, 7605-7622, (2012).

[15] D.-Y. Du, J.-S. Qin, S.-L. Li, Z.-M. Su and Y.-Q. Lan, Chem. Soc. Rev., 13, 4615-4632, (2014).

[16] M. Carraro and S. Gross, Materials, 5, 3956-3989, (2014).

[17] M. Mirzaei, H. Eshtiagh-Hosseini, M. Alipour and A. Frontera, Coord. Chem. Rev., 1-18, (2014).

[18] W.-W. He, S.-L. Li, H.-Y. Zang, G.-S. Yang, S.-R. Zhang, Z.-M. Su and Y.-Q. Lan, Coord. Chem. Rev., 141-160, (2014).

[19] M.-P. Santoni, G. S. Hanan and B. Hasenknopf, Coord. Chem. Rev., 64-85, (2014).

[20] S. Taleghani, M. Mirzaei, H. Eshtiagh-Hosseini and A. Frontera, Coord. Chem. Rev., 84-106, (2016).

[21] J. Zhang, Y. Huang, G. Li and Y. Wei, Coord. Chem. Rev., 395-414, (2019).

[22] P. Ma, F. Hu, J. Wang and J. Niu, Coord. Chem. Rev., 281-309, (2019).

[23] J. Yan, X. Zheng, J. Yao, P. Xu, Z. Miao, J. Li, Z. Lv, Q. Zhang and Y. Yan, J. Organomet. Chem., 1-16, (2019).

[24] N. Belai and M. T. Pope, Chem. Commun., 46, 5760-5762, (2005).

[25] K. Patel and A. Patel, Mater. Res. Bull., 2, 425-431, (2012).

[26] K. Patel and A. Patel, Inorg. Chim. Acta, 79-83, (2012).

[27] A. Patel and K. Patel, J. Coord. Chem., 1-13, (2019).

[28] S. Allenmark, Chirality, 5, 409-422, (2003).

Conclusions

- $PW_{11}Cu$ was successfully functionalized using imidazole, and various spectral characterizations confirmed the formation of chemical bond between $PW_{11}Cu$ and the organic ligand.
- High conversion was a result of synergic effect between imidazole and $PW_{11}Cu$ while high selectivity was attributed to the dual role of imidazole, i.e., radical mechanism initiator as well as Lewis base.
- Further, chirality was successfully induced in $PW_{11}Cu$ by functionalizing it with (*S*)-1-phenylethylamine, and chemical bond formation as well as optical activity were confirmed by various characterizations.
- Good *enantioselectivity* for *S*-styrene oxide with molecular oxygen is obtained, indicating that even a small amounts of chiral ligand, *S*-PEA, can induce chirality into $PW_{11}Cu$.